

Tunable-Combinatorial Mechanisms of Acquired Resistance Limit the Efficacy of BRAF/MEK Cotargeting but Result in Melanoma Drug Addiction

Highlights

- BRAFi+MEKi-resistant melanomas augment mutational mechanisms of BRAFi resistance
- Extreme gene dosage changes or concurrent mutations drive double-drug resistance
- Neophysiologic $V600E$ BRAF- WT CRAF or - MUT MEK interactions can drive MAPK reactivation
- Acute double-drug withdrawal elicits ERK rebound and loss of melanoma viability

Authors

Gatien Moriceau, Willy Hugo, ..., Antoni Ribas, Roger S. Lo

Correspondence

rlo@mednet.ucla.edu

In Brief

Moriceau et al. show that BRAF mutant melanomas acquire resistance to combined BRAF and MEK inhibition by augmenting or combining mechanisms of resistance to single-agent BRAF inhibition, leading to $V600E$ BRAF-CRAF or $V600E$ BRAF- MUT MEK interaction and MAPK pathway reactivation.



Tunable-Combinatorial Mechanisms of Acquired Resistance Limit the Efficacy of BRAF/MEK Cotargeting but Result in Melanoma Drug Addiction

Gatien Moriceau,^{1,7,15} Willy Hugo,^{1,7,15} Aayoung Hong,^{1,2,7,15} Hubing Shi,^{1,7,15} Xiangju Kong,^{1,7} Clarissa C. Yu,^{1,7} Richard C. Koya,⁸ Ahmed A. Samatar,⁹ Negar Khanlou,^{3,7} Jonathan Braun,^{3,6,7} Kathleen Ruchalski,^{4,7} Heike Seifert,¹⁰ James Larkin,¹⁰ Kimberly B. Dahlman,^{11,13} Douglas B. Johnson,^{12,13} Alain Algazi,¹⁴ Jeffrey A. Sosman,^{12,13} Antoni Ribas,^{2,5,6,7} and Roger S. Lo^{1,2,6,7,*}

¹Division of Dermatology, Department of Medicine

²Department of Molecular and Medical Pharmacology

³Department of Pathology and Laboratory Medicine

⁴Department of Radiological Sciences

⁵Division of Hematology and Oncology, Department of Medicine

⁶Jonsson Comprehensive Cancer Center

⁷David Geffen School of Medicine

University of California, Los Angeles, Los Angeles, CA 90095, USA

⁸Division of Oncology, Department of Medicine, Roswell Park Cancer Institute, Buffalo, NY 14263, USA

⁹Discovery Oncology, Merck Research Laboratories, Boston, MA 02115, USA

¹⁰Department of Medicine, Royal Marsden NHS Foundation Trust, London SW3 6JJ, UK

¹¹Department of Cancer Biology

¹²Department of Medicine

¹³Vanderbilt-Ingram Cancer Center

Vanderbilt University, Nashville, TN 37232, USA

¹⁴Division of Hematology and Oncology, University of California, San Francisco, San Francisco, CA 94143, USA

¹⁵Co-first author

*Correspondence: rlo@mednet.ucla.edu

<http://dx.doi.org/10.1016/j.ccell.2014.11.018>

SUMMARY

Combined BRAF- and MEK-targeted therapy improves upon BRAF inhibitor (BRAFi) therapy but is still beset by acquired resistance. We show that melanomas acquire resistance to combined BRAF and MEK inhibition by augmenting or combining mechanisms of single-agent BRAFi resistance. These double-drug resistance-associated genetic configurations significantly altered molecular interactions underlying MAPK pathway reactivation. ^{V600E}BRAF, expressed at supraphysiological levels because of ^{V600E}BRAF ultra-amplification, dimerized with and activated CRAF. In addition, MEK mutants enhanced interaction with overexpressed ^{V600E}BRAF via a regulatory interface at R662 of ^{V600E}BRAF. Importantly, melanoma cell lines selected for resistance to BRAFi+MEKi, but not those to BRAFi alone, displayed robust drug addiction, providing a potentially exploitable therapeutic opportunity.

INTRODUCTION

RAS and *BRAF* are frequently mutated in human malignancies. In advanced melanoma, *NRAS* and, less often, *KRAS* mutations

occur in ~20% of cases and are mutually exclusive with *BRAF* mutations, which are present in ~50% of cases. Somatic *MEK1* or *MEK2* mutations, which can be concurrent with *RAS* or *BRAF* mutations, have also been detected (Hodis et al., 2012;

Significance

The understanding that *BRAF* mutant melanomas frequently acquire BRAFi resistance via MAPK pathway reactivation has guided the development of combined BRAF- and MEK-targeted therapy. Our finding that acquired resistance to BRAF and MEK cotargeting is driven by highly tunable-combinatorial mechanisms of resistance underscores the intrinsic limitation of dual MAPK pathway targeting. Mechanistic studies highlight ^{V600E}BRAF-^{WT}CRAF and ^{V600E}BRAF-^{MUT}MEK interactions as bases for ERK reactivation. Additionally, we demonstrate that melanoma cells with acquired BRAFi+MEKi resistance are exquisitely sensitive to acute drug withdrawal. Exploiting melanoma addiction to BRAFi+MEKi for therapeutic gain is being tested, via intermittent drug dosing, in the clinic (SWOG/CTEP S1320).

Krauthammer et al., 2012; Nikolaev et al., 2012; Shi et al., 2012a), but their roles in pathogenesis and therapeutic responses remain ill defined. *BRAF* mutations strongly predict responses to ATP-competitive BRAF inhibitors (BRAFi) such as vemurafenib and dabrafenib. Allosteric MEK1 and MEK2 inhibitors (MEKi), such as trametinib, selumetinib, cobimetinib, and binimetinib, may have antitumor activities against a broader melanoma segment, including those with *NRAS* mutations or with both wild-type (WT) *NRAS* and WT *BRAF*, but MEKi monotherapy for patients with *BRAF* mutant melanomas is associated with a narrower therapeutic window (versus BRAFi) (Ribas and Flaherty, 2011).

Melanoma regrowth after initial response to MEKi has been attributed to a ^{P124L}*MEK1* mutation (Emery et al., 2009), and acquired MEKi resistance in *BRAF* mutant colorectal cell lines has been linked to a ^{F129L}*MEK1* mutation (Wang et al., 2011) or *BRAF* amplification (Corcoran et al., 2010). How these MEK mutations mechanistically account for MEKi resistance is not entirely clear. Due to the superior clinical benefits of BRAFi for melanoma patients, mechanisms of acquired BRAFi resistance have been studied extensively, and those well validated clinically include *NRAS* or *KRAS* mutations (Nazarian et al., 2010; Shi et al., 2014), ^{V600E}*BRAF* amplification (Shi et al., 2012b) or alternative splicing (Poulidakos et al., 2011; Shi et al., 2012a), *MEK1* or *MEK2* mutations (Shi et al., 2012a; Wagle et al., 2011), *CDKN2A* loss (Shi et al., 2014), and genetic alterations in the phosphatidylinositol 3-kinase-phosphatase and tensin homolog-protein kinase B (PI3K-PTEN-AKT) pathway (Shi et al., 2014; Van Allen et al., 2014). The convergence of multiple mechanisms to reactivate the mitogen-activated protein kinase (MAPK) pathway provided a strong rationale for combined BRAF and MEK targeting to overcome BRAFi resistance, a strategy that is supplanting single-agent BRAFi therapy. However, acquired resistance to BRAFi+MEKi still limits the long-term survival of patients with advanced ^{V600E/K}*BRAF* melanoma. A priori, the intransigence of acquired resistance in response to dual MAPK targeting may be due to preferential emergence of MAPK-redundant resistance pathways. Evidence of branched evolution, extensive inpatient as well as intra- and intertumor heterogeneity, and increased tumor fitness as melanoma emerges from BRAFi-imposed evolutionary selection may help explain why the BRAFi+MEKi combinatorial approach is also an “uphill battle” (Shi et al., 2014).

In this study, we investigate the genetic mechanisms of acquired BRAFi+MEKi resistance and elucidate their signaling consequences and therapeutic implications.

RESULTS

Genetic Alterations Underlying Acquired Resistance to BRAF/MEK Cotargeting in Melanoma

We assembled melanoma tissues with acquired resistance to BRAFi+MEKi (abbreviated as DD-DP for double-drug disease progression) (n = 28 DD-DP tumors, each with patient-matched baseline tumors) from patients (n = 15) treated under two distinct clinical scenarios (Figure 1A): (1) upfront BRAFi+MEKi (dabrafenib+trametinib or vemurafenib+cobimetinib) in patients (n = 10) who were naive to treatment with either BRAFi or MEKi and (2) BRAFi+MEKi (vemurafenib+cobimetinib) in patients (n = 5) who had previously responded to but progressed on BRAFi (vemurafenib) alone (Table S1 available online). We then

analyzed known mechanisms of acquired BRAFi resistance in the MAPK pathway by sequencing the most pertinent exons of *BRAF*, *NRAS*, *KRAS*, *MEK1*, and *MEK2* and performing *BRAF* copy-number analysis (Table S2). Sixteen of 28 DD-DP tumors, along with their patient-matched baseline tumors and normal tissues (n = 7), were whole exome sequenced and analyzed for MAPK and PI3K-PTEN-AKT pathway alterations as reported previously (Shi et al., 2014) (Table S2). In 19 of 28 (68%) DD-DP tumors, we detected known mechanisms of acquired BRAFi resistance in the two core resistance pathways. These included eight DD-DP tumors harboring ^{V600E}*BRAF* amplification, four harboring *NRAS* activating mutations, one harboring a *KRAS* activating mutation, eight harboring *CDKN2A* deletions, three harboring *PTEN* loss-of-function (LOF) mutation (a substitution resulting in F127V; Figure S1) or deletions, and one harboring a *PIK3R1* deletion. In contrast to the same alterations detected in the context of resistance to BRAFi monotherapy (Shi et al., 2014; Van Allen et al., 2014), those associated with acquired BRAFi+MEKi resistance were notable for augmented gene dosage changes, e.g., ^{V600E}*BRAF* ultra-amplification with 74 or 88 copies (Figure 1B; Table S2), LOF ^{F127V}*PTEN* mutation (Figure 1C) or homozygous *PTEN* deletions, ^{G12R}*NRAS* with selective mutant allele amplification (Figures 1D and 1E), and homozygous *CDKN2A* deletions (Table S2). There were examples suggesting combinatorial mechanisms, e.g., concurrent heterozygous ^{Q61K}*NRAS* with homozygous *CDKN2A* deletion and LOF *PTEN* mutation, ^{V600E}*BRAF* amplification concurrent with homozygous *CDKN2A* deletion or hemizygous *DUSP4* deletion (with related ^{V600E}*BRAF* up-expression and *DUSP4* down-expression; Figures 1F–1H); and homozygous *CDKN2A* deletion concurrent with homozygous *PTEN* deletion and hemizygous *PIK3R1* deletion. Thus, genetic analysis of melanomas progressing on BRAFi+MEKi revealed a prevalence of mechanisms of acquired BRAFi resistance, but these genetic alterations often occurred in greater magnitudes or in combinations.

BRAFi-Resistant Melanoma Rapidly Upregulates Resistance Mechanisms Individually or Combinatorially to Overcome BRAF/MEK Inhibitors

To further understand acquired BRAFi+MEKi resistance in melanoma underlying the two aforementioned clinical contexts, we generated isogenic human ^{V600E}*BRAF* melanoma cell lines using treatment regimens mimicking each clinical context. In the sequential resistance model, we took those isogenic sublines with acquired BRAFi (vemurafenib) resistance (single-drug resistance or SDR), via clinically validated mechanisms such as *NRAS* mutation (M249R4) (Nazarian et al., 2010), ^{V600E}*BRAF* alternative splicing (M397R) (Shi et al., 2012b), or amplification (M395R) (Shi et al., 2012b), and generated further sublines with BRAFi+MEKi (vemurafenib+selumetinib) or double-drug resistance (DDR). In the upfront BRAFi+MEKi resistance model, we took the same set of parental (P), drug-naive melanoma cell lines and treated them at the outset with BRAFi+MEKi until we generated sublines with DDR (Figure 2A). The cell subpopulations were exposed to similar increments of inhibitor concentrations, with the duration at each inhibitor concentration dictated by successful population doubling within 3–4 days. When the time-cumulative doses to reach the full DDR phenotype (defined as 2 μ M BRAFi+MEKi) were compared between these two models,

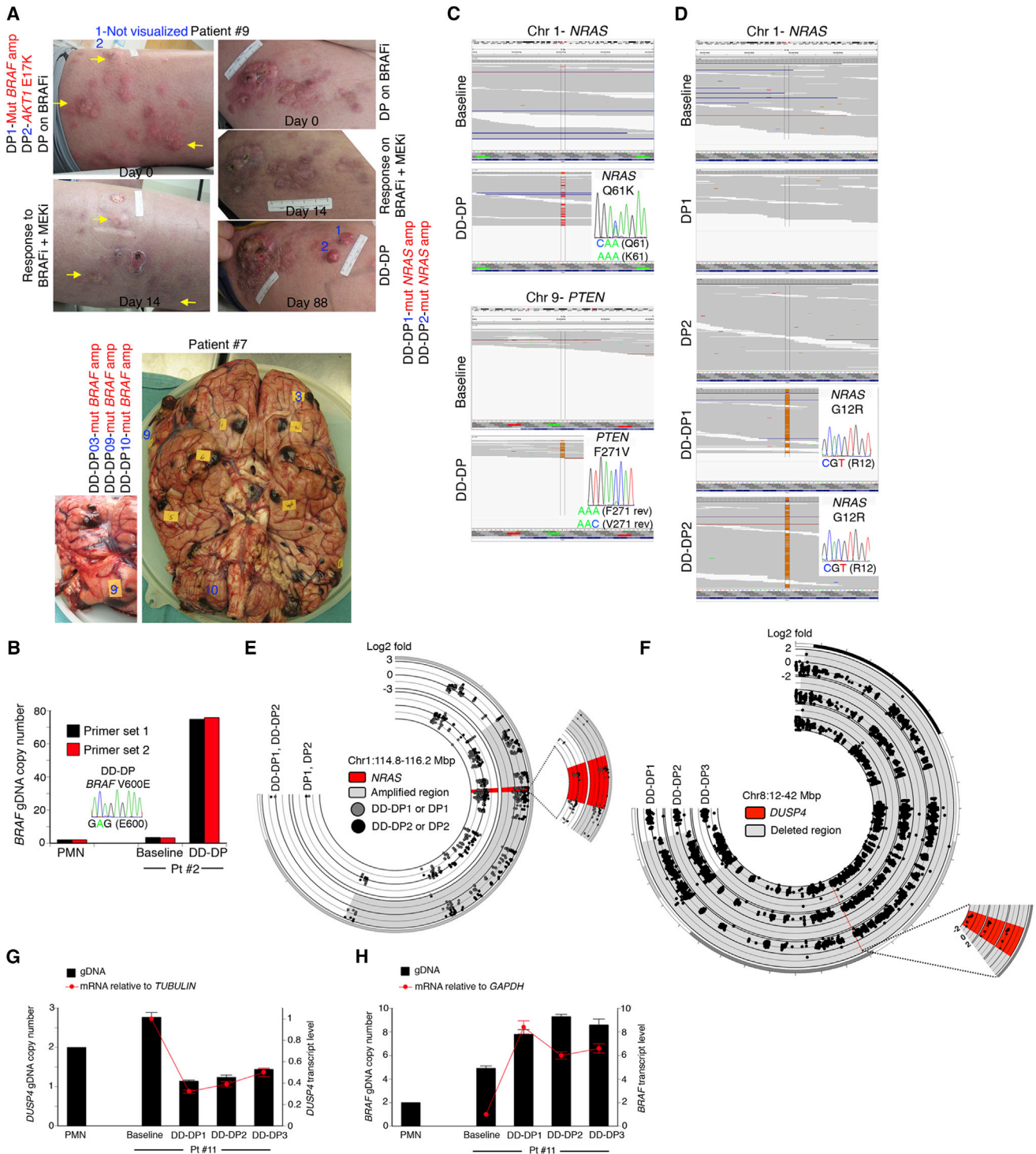


Figure 1. Melanomas Resistant to BRAF/MEK Inhibitors Display Exaggerated Genetic Mechanisms of BRAF Inhibitor Resistance
 (A) Clinical photos denoting specific genetic mechanisms (red) of drug resistance detected within specific tumors (blue). For patient 9, BRAFi-disease progressive melanomas responded to BRAFi+MEKi (yellow arrows) on day 14, with disease progression ensuing as evident on day 88.
 (B) qPCR and Sanger sequencing of gDNAs extracted from melanoma samples from patient 2 and peripheral mononuclear cells (PMN) as a control. The bar graph shows averages of duplicates.
 (C) DD-DP melanoma from patient 6 with concurrent heterozygous ^{Q61K}NRAS (exomeSeq) and compound heterozygous of ^{K197*}PTEN (not shown) and ^{F271V}PTEN (RNASeq). Display by Integrative Genome Viewer with Sanger validation.
 (D) ^{G12R}NRAS homozygosity in patient 9 DD-DP tumors.

(legend continued on next page)

it was clear that the development of DDR from SDR was much faster than DDR directly from P lines (Figure 2A). This observation is consistent with the hypothesis that preexisting mechanisms of BRAFi resistance could be readily augmented or tuned up to confer resistance to BRAFi+MEKi.

To assess this hypothesis, we examined the SDR versus SDR-DDR isogenic pairs of cell lines for alterations in the preexisting, defined mechanisms of BRAFi resistance (Figures 2B–2E). We showed that the M397 SDR→DDR progression was associated with a dramatically upregulated level of alternatively spliced V^{600E} BRAF mRNA (Figure 2B). Moreover, the M395 SDR→DDR progression resulted in further V^{600E} BRAF amplification along with mRNA up-expression. The M249 SDR→DDR progression upregulated mutant NRAS mRNA levels without genomic DNA (gDNA) copy-number gain (Figures 2C and 2D). Accordingly, at the protein expression level (Figure 2E), M249 SDR-DDR expressed an increased NRAS level; M397 SDR-DDR upregulated the level of a truncated p61 V^{600E} BRAF; and M395 SDR-DDR upregulated V^{600E} BRAF expression further (all relative to isogenic SDR sublines). Moreover, full-length V^{600E} BRAF overexpression (in M395 SDR or SDR-DDR) was associated with extensive phospho (p)-CRAF levels (versus their P line). Thus, common mechanisms of acquired BRAFi resistance are highly tunable by either genetic or nongenetic means, and augmentation or combination of such molecular alterations readily confers resistance to BRAFi+MEKi.

We then tested whether specific examples of gene dosage augmentation or concurrent genetic alterations from the exomic analysis of paired melanoma tissues would augment BRAFi+MEKi resistance in cell line models. Parallel to the mutant NRAS amplifications detected in both DD-DPs of patient 9 (Figures 1D and 1E), M249 SDR-DDR up-expressed mutant NRAS (albeit via a nonmutational mechanism) (versus P or SDR) (Figures 2A and 2C–2E). NRAS knockdown (Figure 2F) restored BRAFi sensitivity to M249 SDR, as would be expected, but it also strongly restored BRAFi+MEKi sensitivity to M249 SDR-DDR in both short- and long-term (Figures 2G and 2H) survival assays, indicating that overexpression of mutant NRAS drove DDR. To engineer a DDR cell line mimicking Q^{61K} NRAS heterozygosity+ F^{271V} PTEN/ K^{197*} PTEN compound heterozygous mutations (DD-DP of patient 6; Figure 1C), we took advantage of the PTEN-expressing, Q^{61K} NRAS-driven M238 SDR subline (Figure 2I), which was derived from its V^{600E} BRAF P line by incremental exposures to increasing doses of BRAFi, and stably introduced small hairpin (sh)PTEN. We showed that PTEN knockdown in M238 SDR increased the p-AKT level (Figure 2J) and resistance to BRAFi+MEKi (Figure 2K), indicating that each resistance mechanism (Q^{61K} NRAS and PTEN loss) quantitatively contributed to DDR. Moreover, given that V^{600E} BRAF amplification concurred with hemizygous DUSP4 deletion (DD-DP1 and DD-DP2 of patient 11), we tested whether DUSP4 knockdown (Figure 2L) could confer DDR to the M395 SDR subline, which acquired BRAFi resistance via V^{600E} BRAF amplification. As

seen in Figure 2M, M395 SDR was moderately cross-resistant to BRAFi+MEKi treatments, but loss of DUSP4 expression augmented DDR.

Clonal Analysis Detects Alternative Genetic Configurations in BRAFi+MEKi Resistance Associated with MAPK Reactivation

Previous results indicate that once subclones with specific BRAFi resistance mechanisms have attained clonal dominance, overcoming BRAFi resistance with the added MEKi is at best an uphill battle. We then sought to understand the underlying mechanism(s) of resistance to upfront BRAFi+MEKi (vemurafenib+selumetinib). A polyclonal DDR subline derived from M249 harbored both mutant BRAF ultra-amplification and a MEK1 mutation (F129L) (data not shown). F^{129L} MEK1 had previously been uncovered in a colorectal subline bred to acquire selumetinib resistance (Wang et al., 2011). To understand the individual contributions of V^{600E} BRAF amplification and MEK1 mutation to the DDR phenotype, we retreated the M249 P with increments of BRAFi+MEKi but derived two single-cell-derived M249 DDR subclones, DDR4 and DDR5. In contrast to M249 P, both DDR4 and DDR5 were highly resistant to the growth-inhibitory effect of BRAFi+MEKi in 3-day 3-(4,5-dimethylthiazol-2-yl)-2,5-diphenyltetrazolium bromide (MTT) assays (Figure 3A). In fact, the apparent “growth stimulation” of DDR4 and DDR5 by BRAFi+MEKi treatment was due to a relative loss of their viability in the absence of optimal concentrations of the inhibitors. This “drug addiction” phenomenon was even more profound in long-term clonogenic assays (see Figure 4). SCH772984, an ERK inhibitor (ERKi) and an analog of which is being tested clinically, was inefficient to inhibit the growth of DDR4 or DDR5 by itself but was highly active against M249 P (Figure 3A). In fact, low concentrations of SCH772984 rescued DDR4 and DDR5 from drug addiction, suggesting that suboptimal ERKi dosing to overcome DDR may paradoxically perpetuate DDR fitness. In contrast, ERKi restored BRAFi+MEKi sensitivity to DDR4 and DDR5, consistent with MAPK pathway reactivation as the major mechanism of acquired resistance to upfront BRAFi+MEKi. This was corroborated by analyzing the MAPK pathway status (p-ERK levels) in the M249 triplet (Figure 3B). After plating for 16 hr without both inhibitors, the triplet cell lines were treated with BRAFi+MEKi (1 hr) at increasing concentrations (Figure 3B) or with BRAFi+MEKi (1 μ M) for increasing durations (up to 72 hr) (Figure S2A). Western blot analysis showed that DDR4 and DDR5, compared to M249 P, displayed higher baseline and inhibitor-treated p-ERK levels as well as faster p-ERK recovery in the continued presence of BRAFi+MEKi. Monitoring further upstream for p-MEK and downstream for p-RSK (T573) levels revealed a similarly rapid recovery of the MAPK pathway (Figure S2B).

Consistent with the BRAF protein levels (Figure 3B), we found that DDR4 harbored V^{600E} BRAF ultra-amplification (47.4-fold or >160 copies), while DDR5 harbored low copy-number

(E) Circos plot showing NRAS copy-number gains in patient 9 DD-DP tumors.

(F) Circos plot showing hemizygous DUSP4 deletions in all three DD-DP tumors from patient 11.

(G and H) DUSP4 (G) and BRAF (H) gDNA copy numbers and mRNA expression levels by qPCR and qRT-PCR, respectively, in tumors from patient 11. Error bars show \pm SD.

See also Figure S1 and Tables S1 and S2.

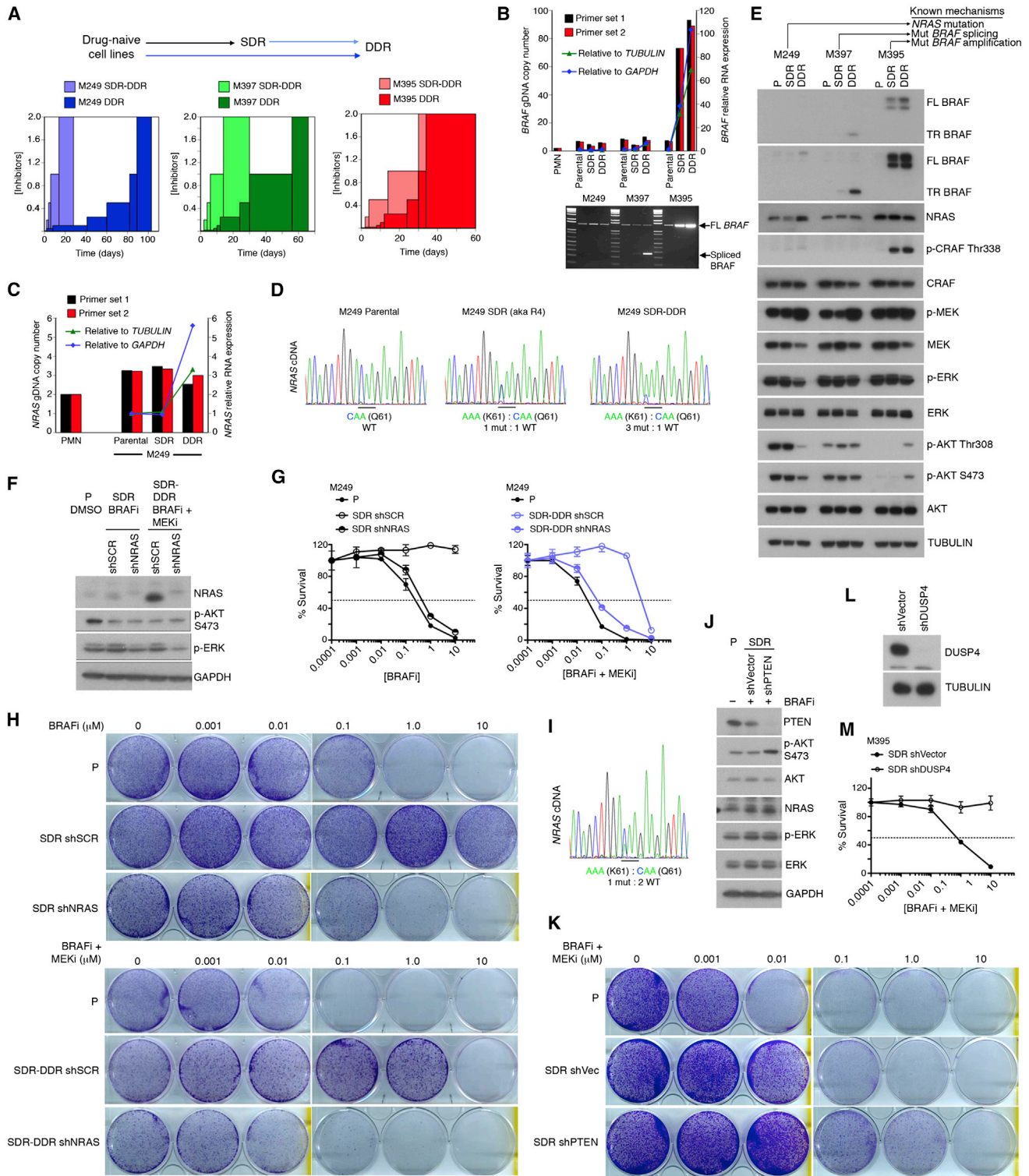


Figure 2. Melanoma Cells with Acquired BRAFi Resistance Further Resist BRAFi+MEKi by Augmenting Existing or Combining Distinct Mechanisms

(A) Relative drug exposure times required to achieve resistance to BRAFi+MEKi in three isogenic groups of ^{V600E}BRAF melanoma cell lines comparing progression from SDR→DDR versus P→DDR. [inhibitor], 0.1–2.0 μM.

(B) gDNA and cDNA BRAF copy numbers (average of duplicates) by qPCR or qRT-PCR (top) and by semiquantitative PCR (bottom).

(C) gDNA and cDNA NRAS levels in the M249 P, SDR, and SDR-DDR cell lines in (A) and (B).

(legend continued on next page)

$V^{600E}BRAF$ gain (4.6-fold or 20 copies) along with $F^{129L}MEK1$ (Figures 3C and 3D). $V^{600E}BRAF$ copy-number gains quantified by gDNA quantitative (q)PCR were corroborated by Sanger sequencing, which showed a *BRAF* mutant-to-WT ratio of 2:1 in the P line (or about three *BRAF* copies) and apparent $V^{600E}BRAF$ homozygosity in DDR4 and DDR5 resulting from selective $V^{600E}BRAF$ amplification (Figure 3D). Moreover, whole exome sequence (WES) analysis of the M249 triplet cell lines confirmed that the DDR-associated altered mutant or variant allelic frequencies (MAFs) of $V^{600E}BRAF$ and $F^{129L}MEK1$ (Figure 3E) were likely due to mutant allele-selective copy-number gains (Figure 3F). WES analysis also detected a low $F^{129L}MEK1$ MAF (4%) in the P polyclonal line, suggesting preexistence of this drug-resistant subclone (Figure 3E). In addition, copy-number variation (CNV) analysis revealed distinct *BRAF* amplicons in M249 DDR4 versus DDR5, suggesting convergent evolution (Figure 3F, top). Since the concurrence of $V^{600E}BRAF$ amplification and $F^{129L}MEK1$ in M249 DDR5 could be selected by distinct inhibitor concentrations, we derived two additional M249 DDR sublines (M249 DDR2 and M249 DDR3) by treatments from the outset with a higher concentration of BRAFi+MEKi (0.5 μ M). In a pattern suggestive of convergent evolution, both M249 DDR2 and DDR3 displayed low copy-number gains of both $V^{600E}BRAF$ and $F^{129L}MEK1$ (Figures S2C–S2E).

Using a $WTBRAF$ cell line, human embryonic kidney 293T (HEK293T) cells, we then tested the impact of MEK mutants associated with MAPK inhibitor (MAPKi) resistance on cellular substrate levels (i.e., p-ERK) and the p-ERK half-maximal inhibitory concentration (IC₅₀) of MEKi (Figures S2F and S2G). We overexpressed $F^{129L}MEK1$, $C^{121S}MEK1$ (which confers BRAFi resistance) (Wagle et al., 2011), and several MEK mutants ($Q^{56P}MEK1$, $K^{59del}MEK1$, and $E^{203K}MEK1$) associated with clinical resistance to MAPK targeting and compared their impacts on baseline p-ERK levels as well as the sensitivities of p-ERK to MEKi (selumetinib). Although overexpression of these MEK1 mutants (versus $WTMEK1$) variably increased the baseline p-ERK level, their cellular p-ERK IC₅₀ value to MEKi did not differ appreciably, arguing against allosteric MEKi binding defect as the shared mechanism of action of MEK mutants. Their concurrence with $V^{600E}BRAF$ amplification argues for a possible cooperative biochemical mechanism of resistance.

To further understand the impact of ERKi on survival of DDR4 and DDR5 cells (Figure 3A), we withdrew DDR4 and DDR5 (16 hr off) from BRAFi+MEKi and then treated them with either ERKi (1 hr) alone or BRAFi+MEKi+ERKi (1 hr) (Figure 3G). ERKi alone was ineffective at suppressing the p-ERK rebound following double-drug withdrawal (Figure 3G). However, once BRAFi+MEKi was reintroduced, additional treatment with ERKi was highly effective in suppressing the p-ERK levels (Figure 3G). Thus, ERKi treatment alone of some melanoma cells previously selected for resistance by BRAFi+MEKi would be ineffective unless very high ERKi doses were delivered, which is unlikely achievable clinically. Thus, clonal M249 DDR4 and DDR5 melanoma sublines harbor salient but distinct genetic alterations that represent tunable and combinatorial modes of resistance to BRAFi+MEKi reversible by combining ERKi.

Distinct Mechanisms of Resistance Driven by $V^{600E}BRAF$ Ultra-amplification or $V^{600E}BRAF$ Amplification+ $F^{129L}MEK1$

Earlier, we noted a robust upregulation of p-CRAF in the M395 SDR and SDR-DDR sublines that harbor $V^{600E}BRAF$ amplification (Figure 2E). Hence, we probed the p-CRAF levels in the M249 triplet lines. DDR4 and DDR5, freshly treated with BRAFi+MEKi (1 hr), displayed robustly elevated p-CRAF levels (DDR4 > DDR5 >> P; Figure 3H). Upregulated p-CRAF levels in DDR4 and DDR5 did not require the continued presence of both inhibitors, as their withdrawal for up to 20 hr after an overnight (16 hr) treatment did not diminish the p-CRAF levels (Figure S2H). We hypothesized that this strong CRAF upregulation in DDR4 (and a weaker upregulation in DDR5) may be driven by supraphysiologic $V^{600E}BRAF$ overexpression, the degree of which positively correlated with that of p-CRAF upregulation (Figures 3B, 3H, and 4A). To test this hypothesis, we knocked down BRAF levels in DDR4 and DDR5, with or without BRAFi+MEKi, and we found that BRAF knockdown effectively downregulated p-CRAF levels (Figure 4A). BRAF knockdown also reduced p-CRAF levels in the $V^{600E}BRAF$ -amplified M395 SDR-DDR subline (Figure 2B; Figure S3A). We also knocked down CRAF directly (Figure 4B) and tested the individual contributions of BRAF versus CRAF to the clonogenic (i.e., long-term) growth and survival of the M249 triplet (Figure 4C). As expected, M249 P growth and survival was not sensitive to CRAF knockdown but highly sensitive

(D) Sanger sequencing of cDNAs from cell lines in (C) with chromatograms showing detection of the WT versus mutant *NRAS* transcripts (ratio estimated by peak heights).

(E) Western blot (WB) of indicated total and phosphoprotein levels from three isogenic triplets (SDR sublines annotated with known BRAFi resistance mechanisms. FL, full length; TR, truncated; TUBULIN, loading control. Treatments with BRAFi (SDR) or BRAFi+MEKi (DDR) (1 μ M), 16 hr prior to lysate preparation. BRAF WB, both short and long exposures shown. Quantification of WBs for NRAS (M249 triplet): 1, 0.98, 1.65; for p61 BRAF (M397 triplet): 1, 2.55, 7.33; and for FL BRAF (M395 triplet): 1, 10.89, 13.63 (normalization to TUBULIN and then P cell line data values set at 1).

(F) NRAS knockdown in the M249 SDR and SDR-DDR lines by shRNA as shown by WB 72 hr after lentiviral infections. Inhibitors were at 1 μ M each. shSCR, shScrambled.

(G) Three-day MTT assays using M249 cell lines from (F). [inhibitor] in micromolar.

(H) Ten-day clonogenic assays using M249 cell lines from (F). BRAFi or BRAFi+MEKi treatments every 2 days were started 24 hr after plating.

(I) cDNA Sanger sequencing showing WT versus mutant *NRAS* transcripts and the estimated ratio in M238 acquired resistant (AR) (SDR) cells.

(J) Stable knockdown of PTEN by lentiviral shRNA in M238 AR (SDR) (BRAFi, 1 μ M) showing the levels of indicated phosphoproteins and total proteins by WB of cellular lysates 72 hr posttransduction, compared to protein levels in the M238 P cell line treated with DMSO. GAPDH, loading control.

(K) Long-term clonogenic assays of indicated cells from (J).

(L) WB showing the DUSP4 protein levels in control and stable knockdown M395 SDR.

(M) Three-day MTT assays of indicated cells from (L).

Error bars show \pm SEM; n = 5; normalized to DMSO as 100%. BRAFi, vemurafenib; MEKi, selumetinib.

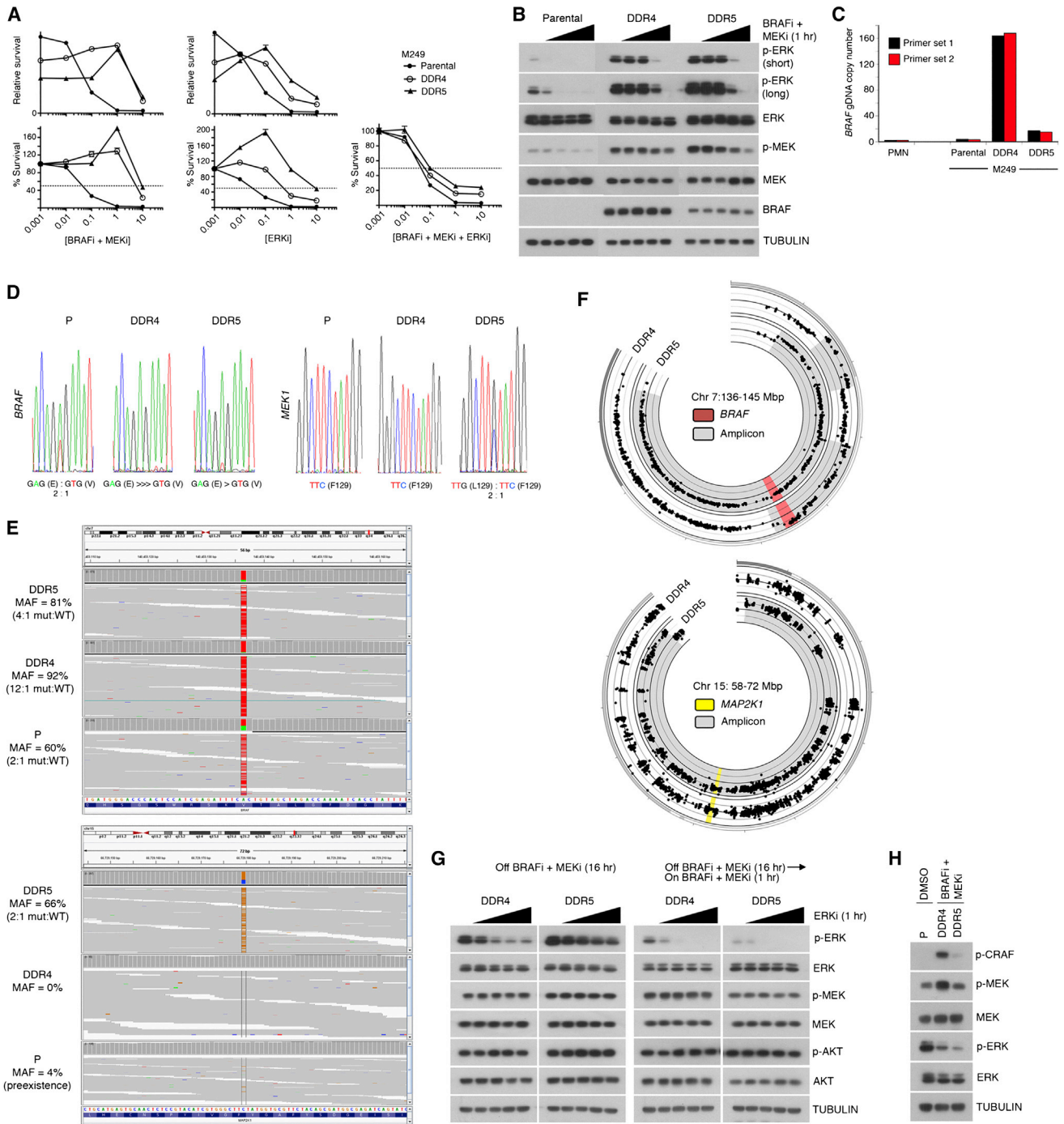


Figure 3. Melanoma Cells Clonally Develop Resistance to Upfront BRAFi+MEKi via Alternative Genetic Configurations

(A) Three-day MTT assays (error bars show \pm SEM, $n = 5$; top, relative raw values; bottom, normalized to DMSO vehicle as 100%). Cells were plated 16 hr without inhibitors prior to treatment with indicated inhibitor(s) (in micromolar).

(B) WB of indicated total and phosphoproteins. M249 cell lines were plated 16 hr without inhibitors prior to BRAFi+MEKi treatments for 1 hr (0–10 μ M in 10-fold increments). TUBULIN, loading control.

(C) *BRAF* copy number by gDNA qPCR (averages of duplicates).

(D) Sanger sequencing showing *BRAF* and *MEK1* mutational status of M249 cell lines.

(E) Integrated Genome View snapshots of reference and mutant reads centered on the A-to-T mutation (chromosome 7:140453136; ^{V600E}*BRAF*) and on the C-to-G mutation (chromosome 15:66729179; ^{F129L}*MEK1*) in indicated M249 cell lines. Mutat:WT ratios estimated from the MAFs. Note a low MAF of ^{F129L}*MEK1* in M249 P.

(legend continued on next page)

to BRAF knockdown. Consistent with prior short-term assays (Figure 3A), both M249 DDR4 and DDR5 displayed dramatic drug addiction. Importantly, in the presence of both inhibitors, the growth and survival of DDR4 and DDR5 were highly dependent on either CRAF or BRAF, suggesting functional and physical interaction.

To assess whether there are likely additional genetic underpinnings of p-CRAF upregulation (and DDR) in DDR4 and DDR5, we analyzed the phylogenetic relationship of the M249 triplet (Figure 4D) and assessed the genetic alterations shared by DDR4 and DDR5 (Table S3). From this WES-based phylogeny, it was apparent that DDR4 and DDR5 single-cell clones represent minor subclones in the P, polyclonal population, since they each harbored a large number of private mutations, which escaped detection in the mixed P population. In fact, the number of shared genetic alterations between DDR4 and DDR5 was exceedingly small (Table S3), suggesting that these few alterations (aside from $V600E$ BRAF amplification) were unlikely drivers of DDR. As the M249 P majority population did not harbor the DDR4- or DDR5-private mutations, we reasoned that the ability of salient genetic features shared by DDR2, DDR3, DDR4, and DDR5 ($V600E$ BRAF amplification) and by DDR2, DDR3, and DDR5 ($F129L$ MEK1 and its low copy-number gain) to reconstitute DDR (and their biochemical features) in M249 P would establish sufficiency (in light of necessity established earlier).

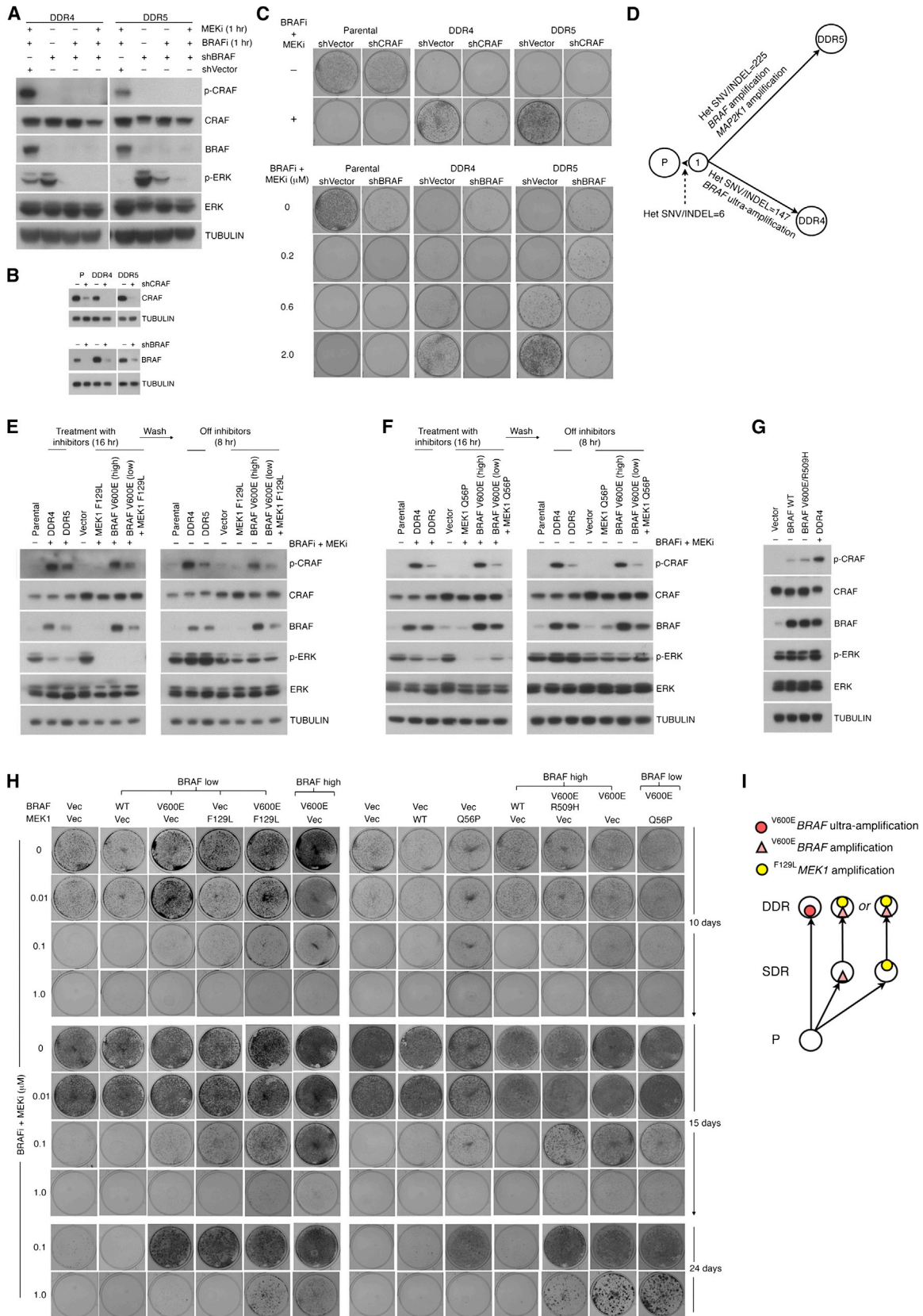
We then directly tested whether supraphysiologic $V600E$ BRAF overexpression, mimicking the DDR4 and DDR5 levels, would be sufficient to upregulate p-CRAF levels. We engineered the M249 P to express stably and homogeneously the empty vector, $F129L$ MEK1 (Figure 4E), or $Q56P$ MEK1 (Figure 4F), $V600E$ BRAF high overexpression, and $V600E$ BRAF low overexpression concurrent with a MEK1 mutation. Regardless of double-drug treatment (16 hr) or subsequent withdrawal (8 hr), $V600E$ BRAF high overexpression induced a robust DDR4-like p-CRAF level, while $V600E$ BRAF low overexpression concurrent with an MEK1 mutation induced a lower, DDR5-like p-CRAF level. Neither vector control nor MUT MEK1 alone had any impact on the p-CRAF level. Also, supraphysiologic expression of WT BRAF or $V600E/R509H$ BRAF (known to disrupt BRAF-CRAF dimerization) in M249 P only marginally upregulated p-CRAF (Figure 4G). However, the M249 P engineered cell lines (versus the spontaneously resistant DDR4 and DDR5 sublines), displayed a slower p-ERK recovery (with or without BRAFi+MEKi; Figures 4E and 4F). This difference (a few hours) was minimal compared to the extremely slow p-ERK recovery observed in the P line (not detectable by 3 days; Figure S2A) and appeared to be due to prior MAPKi exposure or preconditioning, which abolished the small difference in the p-ERK recovery rate between the M249 P engineered lines versus DDR4 and DDR5 (Figure S3B).

We then assessed the relative potencies of individual alterations observed in M249 DDR4 and DDR5 to confer BRAFi+MEKi resistance in M249 P using both short-term (Figures S3C and S3D) and long-term (Figures 4H) survival assays. $V600E$ BRAF

high overexpression or $V600E$ BRAF low overexpression concurrent with MEK1 mutant ($F129L$ or $Q56P$) conferred more than one-log (short-term) or two-log (long-term) increases in MAPKi resistance. Interestingly, preconditioning of the engineered M249 lines conferred double-drug addiction (Figures S3E and S3F). As was noted previously for DDR4 and DDR5 sublines (Figures 3A and 4C), the double-drug addiction phenotype also exaggerated the apparent DDR phenotype of preconditioned M249 P engineered with each genetic configuration (Figure S3D). These data together (Figures 4E and 4F; Figures S3B–S3F) thus suggest a mechanistic link between double-drug addiction and p-ERK rebound (see below in Figure 7). Moreover, supraphysiologically expressed $V600E/R509H$ BRAF, defective in p-CRAF induction (Figure 4G), was also compromised in its ability to resist repeated treatments with BRAFi+MEKi (1 μ M, 24 days). $V600E$ BRAF low overexpression or MEK1 mutation alone was individually able to confer BRAFi+MEKi resistance, but only to an extent appreciably weaker than achieved by their combination (see growth at 0.1 versus 1.0 μ M of drugs at days 15 and 24) (Figure 4H). The combinatorial effects of overexpressed $V600E$ BRAF and MEK1 mutants on promoting the DDR phenotype could also be observed in a different cell line (Figures S3G–S3I). Thus, ERKi-sensitive, acquired resistance to BRAFi+MEKi observed in DDR4 and DDR5 is causally attributable to either supraphysiologic overexpression of $V600E$ BRAF or a lower degree of $V600E$ BRAF and MUT MEK overexpression (Figure 4I; Figure S3). Mechanistically, excess $V600E$ BRAF proteins promote dimerization with CRAF as well as CRAF activation and dependency.

Next, to dissect mechanistically how MUT MEK1 aids overexpressed $V600E$ BRAF in establishing a full DDR phenotype, we posited that overexpressed $V600E$ BRAF and MUT MEK physically and functionally interact in a complex facilitated by (1) the MEK mutant conformation and (2) a kinase-independent regulatory role of $V600E$ BRAF. This complex would facilitate MEK phosphorylation and activation by CRAF, akin to a modeled MEK-KSR2-BRAF regulatory complex (Brennan et al., 2011). Hence, we tested whether $F129L$ MEK1 in DDR5, but not DDR4, would be more abundantly associated physically with $V600E$ BRAF. Accordingly, we immunoprecipitated BRAF in the M249 triplet and probed for MEK1 and MEK2 in the immunoprecipitates. Consistently, much more MEK1 and MEK2 were detected in complex with BRAF in $F129L$ MEK1-harboring DDR5 (Figure 5A). We then specifically immunoprecipitated MEK1 and detected a dramatically higher BRAF level bound to MEK1 in DDR5 (Figure 5B). However, the pattern of BRAF-MEK2 binding was reversed; we detected more BRAF bound to MEK2 in DDR4 (Figure 5C). MEK2 in DDR4 was also associated with the highest level of activation-associated phosphorylation at S226, consistent with MEK2 recruitment to and activation by a BRAF-containing complex. Under the same conditions, we were unable to detect CRAF or KSR2 in BRAF, MEK1, or MEK2 immunoprecipitates (data not shown). These data suggest that the supraphysiologic level of $V600E$ BRAF in DDR4 recruits both WT MEK1 and WT MEK2,

(F) CNV display by Circos (with respect to M249 P) showing distinct BRAF amplicons in DDR4 versus DDR5 (top) and MEK1 copy-number gain in DDR5 (bottom). (G and H) WB of indicated total and phosphoproteins from M249 cell lines plated 16 hr without inhibitors prior to ERKi treatments for 1 hr (0–10 μ M) without or with BRAFi+MEKi cotreatment (1 μ M) (G) or prior to BRAFi+MEKi treatment (1 μ M, 1 hr) (H). BRAFi, vemurafenib; MEKi, selumetinib; ERKi, SCH722984. See also Figure S2.



(legend on next page)

whereas the $V600E$ BRAF level overexpressed to a lesser extent in DDR5 recruits $F129L$ MEK1 preferentially over WT MEK2.

We also assessed the relative phosphorylation status of MEK1 and MEK2 in DDR4 and DDR5 16 hr after treatment with BRAFi+MEKi versus M249 P treated with DMSO. Interestingly, we observed that only DDR4, but not DDR5, harbored an enhanced level of activation-associated MEK1 and MEK2 phosphorylation (Figure 5D). In both DDR4 and DDR5, MEK1 displayed increased levels of ERK-dependent negative feedback phosphorylation on T291 within its proline-rich region of the kinase domain, which was not present on MEK2, suggesting that the time-cumulative ERK activities are far greater in DDR4 and DDR5 despite BRAFi+MEKi treatment than in P M249. DDR5 harbored the highest level of p-MEK1 T291, which has been shown to reduce MEK1-MEK2 heterodimerization and MEK2 S226 phosphorylation (Catalanotti et al., 2009) and may also explain the reduced p-MEK1 S222 level (Figures 5D).

We then sought to reconstitute $F129L$ MEK1- $V600E$ BRAF interaction and its functional role in DDR. We had observed that the majority of MEK1 and MEK2 mutations thus far detected specifically in melanomas with clinically acquired BRAFi, MEKi, or BRAFi+MEKi resistance (Emery et al., 2009; Shi et al., 2014; Van Allen et al., 2014; Villanueva et al., 2013; Wagle et al., 2011, 2014) cluster three dimensionally in or proximal to helices A and C (Figure 5E; Movie S1). Specifically, in M249 P, we minimally overexpressed a series of FLAG-tagged MEK1 constructs and coexpressed either hemagglutinin (HA)-tagged WT BRAF or $V600E$ BRAF, both at high levels akin to DDR5 (Figures 5F and S4). We then immunoprecipitated protein complexes via FLAG and detected MEK1, BRAF, and HA levels. Importantly, both $F129L$ MEK1 and $Q56P$ MEK1, which is homolog to $Q60P$ MEK2, displayed dramatically enhanced and preferential interaction with overexpressed $V600E$ BRAF relative to WT MEK1. Anti-BRAF signals detected in the FLAG immunoprecipitates presumably contained both endogenous and exogenous $V600E$ BRAF. Thus, these data support the notion that BRAFi+MEKi treatment in melanoma selects for MEK1 or MEK2 mutations that impact a discrete structural subdomain and leads to a conformation favoring physical association with overexpressed $V600E$ BRAF.

To assess the functional relevance of a $V600E$ BRAF- MUT MEK complex, we searched for clues of a BRAF-MEK physical interaction interface (Figure S5). Based on prior structural data

of MEK1-BRAF (Haling et al., 2014), vemurafenib-bound $V600E$ BRAF (Bollag et al., 2010), and MEK1-KSR2 (Brennan et al., 2011) and structural alignments of vemurafenib-bound $V600E$ BRAF with BRAF or KSR2, we hypothesized a regulatory $V600E$ BRAF- MUT MEK complex where $V600E$ BRAF R662 makes critical contacts with MEK residues in one complex interface (Figures 6A and 6B). We predicted that the R662L substitution in $V600E$ BRAF would disrupt this face-to-face $V600E$ BRAF- MUT MEK interaction and attenuate the DDR phenotype. Ectopic expression of vector, HA- WT BRAF, HA- $V600E$ BRAF, and HA- $V600E/R662L$ BRAF in WT BRAF HEK293T cells revealed that the R662L substitution did not interfere with the $V600E$ BRAF kinase activation status in the absence of MAPKi (Figure 6C). We then engineered M249 P to stably express a FLAG- $F129L$ MEK1 or FLAG- $Q56P$ MEK1 along with HA-tagged WT or various mutant BRAF at levels akin to M249 DDR5 (Figure 6D). After BRAFi+MEKi treatment (1 μ M, 16 hr), anti-FLAG immunoprecipitation followed by western blots revealed that both MEK1 mutants most abundantly interacted with $V600E$ BRAF, consistent with previous results (Figure 5F). Importantly, the R662L mutation in the context of $V600E$ BRAF strongly abolished this enhanced $V600E$ BRAF- MUT MEK1 complex and reduced the overall p-ERK levels. $V600E/R509H$ BRAF also appeared to display reduced interaction with MUT MEK1 but without a reduction in the p-ERK levels, suggesting that this apparent reduction was due to loss of BRAF dimers (Figure 6A) (Haling et al., 2014) or higher-order oligomers (Nan et al., 2013) brought down by anti-FLAG. Consistently, whereas engineered M249 P lines highly overexpressing $V600E$ BRAF or minimally overexpressing $V600E/R509H$ BRAF together with a MEK1 mutant were able to resist robustly BRAFi+MEKi at 1 μ M, those cell lines expressing $V600E/R662L$ BRAF or WT BRAF along with an MEK1 mutant grew poorly over 28- or 32-day treatments with BRAFi+MEKi (Figure 6E). Taken together, these studies (Figures 4, 5, and 6; Figures S3–S5) highlighted a critical role of upstream MAPK reactivation, i.e., upregulation of the $V600E$ BRAF-CRAF-MEK complex, in the MAPKi resistance phenotype. Buildup of this plastic complex is dependent on the degree of BRAF and/or MEK inhibition and likely other cell context determinants. In the extreme case of DDR, alternative mechanisms to upregulate this complex can be achieved by $V600E$ BRAF (variably overexpressed) interacting with WT CRAF or with MUT MEK.

Figure 4. Achieving BRAF/MEK Inhibitor Resistance via Tuning $V600E$ BRAF Gene Dosage with or without MEK Mutations

(A) M249 DDR4 and DDR5 plated 16 hr with BRAFi+MEKi (1 μ M each), transduced with lentiviral shVector or shBRAF for 48 hr, and treated with (+) or without (–) inhibitors at 1 μ M (1 hr) were analyzed by WB. TUBULIN, loading control.

(B) WB for CRAF or BRAF in M249 triplet 48 hr after without (–) or with (+) CRAF or BRAF knockdown, as indicated.

(C) Cells from (B) plated for clonogenic assays.

(D) Whole exome-based phylogenetic relationships of the M249 triplet cell lines. Branch lengths proportional to the number of heterozygous (het) SNVs and small INDELs private to each cell line with respect to the theoretical common ancestral cell subpopulation (1). The DDR-unique copy-number variations of indicated genes also shown.

(E and F) WB of total and phosphoprotein levels in M249 triplet and M249 P engineered to express $V600E$ BRAF and $F129L$ MEK1 (E) or $Q56P$ MEK1 (F). Selected cell lines treated with BRAFi+MEKi (1 μ M) for 16 hr and then washed free of inhibitors for 8 hr.

(G) WB analysis of M249 P engineered to express vector, WT BRAF, or $V600E/R509H$ BRAF (without inhibitors) or M249 DDR4 (BRAFi+MEKi, 1 μ M, 16 hr).

(H) Clonogenic assays of M249 P engineered to express the indicated levels of WT versus mutant BRAF and/or MEK1 and their relative resistance to BRAFi+MEKi over inhibitor concentrations and time.

(I) Temporal genetic clonal evolution of MAPKi resistance with magnitudes matching graded selective pressures and with augmented gene dosage versus combinatorial genetic alterations proposed as distinct pathways. Distinct $V600E$ BRAF amplicons indicative of convergent evolution. Each circle, dominant subclone.

BRAFi, vemurafenib; MEKi, selumetinib. See also Figure S3 and Table S3.

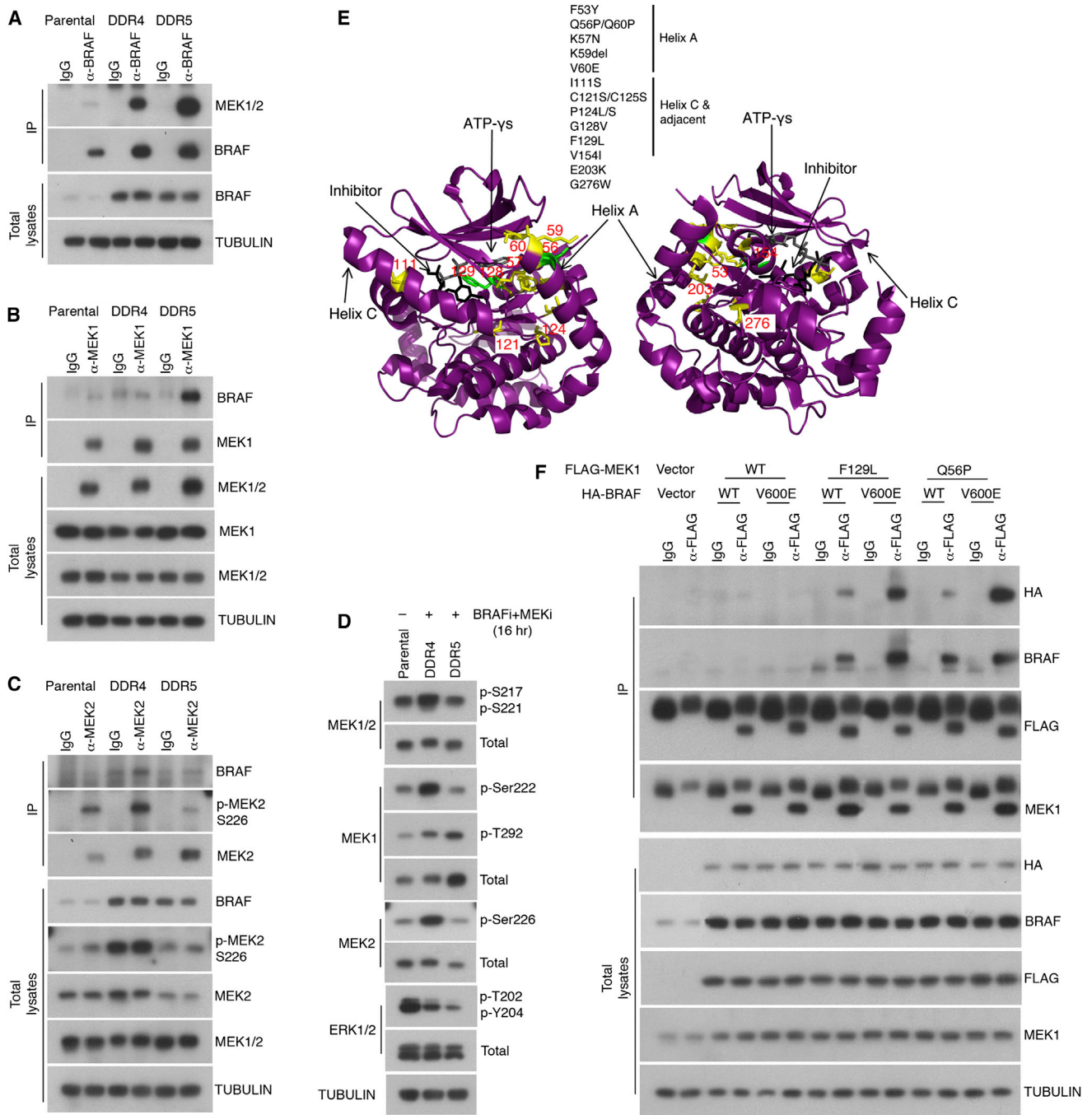


Figure 5. Distinct MEK Mutants Share Enhanced Interaction with ^{V600E}BRAF

(A–C) The M249 triplet cell lines were plated without (P) or with (DDR4 and DDR5) BRAFi+MEKi (1 μ M, 16 hr), and lysates were subjected to immunoprecipitation (IP) using a control antibody (immunoglobulin G [IgG]) or BRAF (A)-, MEK1 (B)-, or MEK2 (C)-specific antibodies. The IP and total fractions were probed by WB. TUBULIN, loading control.

(D) WB analysis of total and p-MEK1 and -MEK2 and -ERK levels in the M249 triplet cell lines.

(E) Structure of MEK1 (two views, 180° rotated) with the locations of MEK1 mutations, or residues homologous to MEK2 mutations, indicated in yellow, except that Q56 and F129 are indicated in green. All mutations, except I111S and P124S, have been detected in melanomas with clinically acquired MAPKi resistance.

(F) M249 P engineered to express vector or FLAG-^{WT}MEK1, FLAG-^{F129L}MEK1, or FLAG-^{Q56P}MEK1 concurrent with overexpression of either HA-^{WT}BRAF or HA-^{V600E}BRAF were plated with BRAFi+MEKi (1 μ M, 16 hr; except vector control), and the lysates were subjected to IP (anti-IgG or -FLAG). WB of IP and total fractions.

BRAFi, vemurafenib; MEKi, selumetinib. See also Figure S4 and Movie S1.

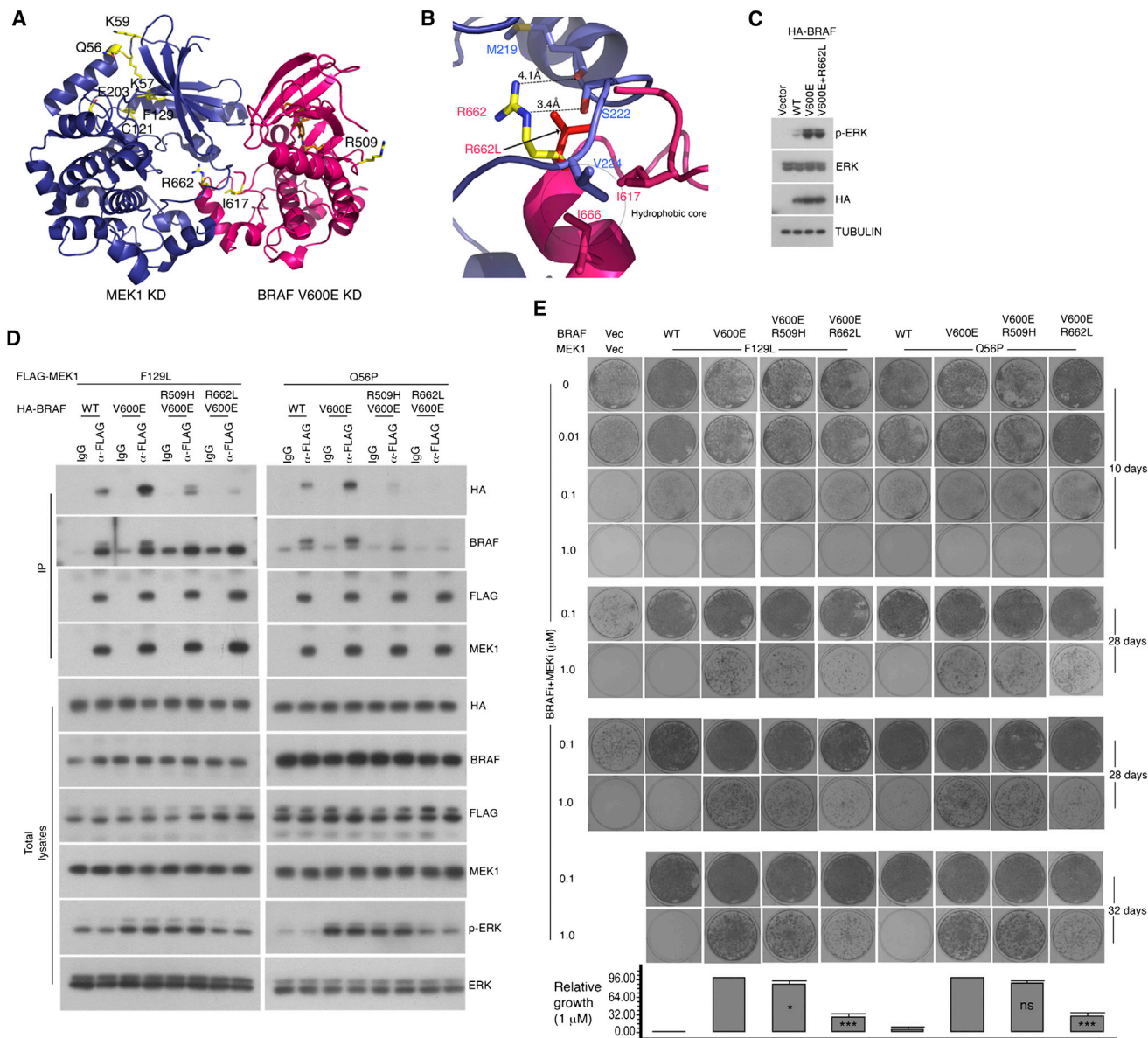


Figure 6. A BRAF-MEK Interface Critical for $V600E$ BRAF- MUT MEK1 Interaction and Cooperative DDR

(A) A predicted MEK1 kinase domain (KD)- $V600E$ BRAF KD complex with yellow color highlighting the locations of (1) MEK1 residues mutated in melanomas with acquired MAPKi resistance; (2) $V600E$ BRAF R509, critical for RAF-RAF dimerization; (3) $V600E$ BRAF R662, structurally homologous to KSR2 A879 critical for MEK1-KSR2 interaction; and (4) $V600E$ BRAF I617, critical for MEK-BRAF dimerization.

(B) Zoomed-in details of MEK1- $V600E$ BRAF interfaces, highlighting MEK1 activation segment residues (blue: M219, S222, and V224) interacting with $V600E$ BRAF R662 (yellow), I617 (magenta), and I666 (magenta) and interactions predicted to be abolished by an R662L (red) mutation.

(C) WB of indicated proteins in HEK293T cells transfected with vector or indicated HA-tagged BRAF constructs. TUBULIN, loading control.

(D) M249 P engineered to moderately overexpress HA-BRAF or the indicated BRAF mutants along with either FLAG-MEK1 mutant (F129L or Q56P). Experiments were performed as described for Figure 5F.

(E) Clonogenic assays of M249 P engineered to express WT or indicated mutant BRAF, MEK1 mutants, and/or their empty vectors (Vec). Relative resistance to BRAFi+MEKi assessed over the indicated concentration range and time points. Three repeats (for 0.1 and 1.0 μ M) are shown for the longest time points (28 and 32 days), and growths were quantified (1 μ M; n = 3; normalization relative to $V600E$ BRAF- MUT MEK1-transduced cells as 100%; means \pm SDs; *p < 0.05, ***p < 0.001, ns, not significant based on ANOVA). BRAFi, vemurafenib; MEKi, selumetinib.

See also Figure S5.

Melanoma Cells with Acquired Resistance to BRAFi+MEKi Display Exquisite Dual Drug Addiction

It has been reported recently that patient-derived xenografts with acquired resistance to BRAFi driven by $V600E$ BRAF ampli-

fication or RNA overexpression could potentially be counterselected during periods of BRAFi withdrawal (Thakur et al., 2013). We thus tested the degree to which M249 DDR4 and DDR5 were addicted to each (BRAFi or MEKi) or both (BRAFi+MEKi)

inhibitors during long-term clonogenic growth. Three days after seeding, DDR4 and DDR5 cells were kept continuously on both inhibitors, washed from both, or replenished with only one of the two inhibitors. Both DDR4 and DDR5 were strongly addicted to continuous treatment with BRAFi+MEKi (Figure 7A). The loss of viability after acute BRAFi+MEKi washout could not be rescued by a dose of ERKi (1 μ M) sufficient to strongly suppress the rebound in p-ERK resulting from drug withdrawal (Figure 7B; Figure S6A). Additionally, this “high” dose of ERKi could resensitize DDR4 and DDR5 to either BRAFi or BRAFi+MEKi, consistent with prior short-term MTT results (Figure 3A). Notably, the antigrowth and antisurvival effect of double-drug withdrawal was comparable to that of ERKi alone or ERKi plus BRAFi (Figure 7B). However, ERKi at a suboptimal dose (0.1 μ M), which could suppress the rebound p-ERK levels induced by acute double-drug withdrawal (Figure S6B), completely rescued the antigrowth and antisurvival effects of BRAFi+MEKi withdrawal and partially “erased” the antigrowth and antisurvival effects of single BRAFi or MEKi withdrawal (Figure 7C). Importantly, a suboptimal dose of ERKi could be antigrowth and antisurvival only if DDR4 and DDR5 were continuously treated with BRAFi+MEKi. We then sought evidence consistent with melanoma regression in patients who have been discontinued on MAPK-targeted therapies due to disease progression or acquired drug resistance. From evaluable patients with melanoma who were treated with BRAFi+MEKi (n = 15) or single-agent BRAFi (n = 16) therapies (Table S4), we retrospectively collated radiologic images before and/or during disease progression and compared them to images, when available or feasible, after a variable time off therapies (Figures S6C and S6D). Although specific clinical examples of tumor regression after cessation of BRAFi+MEKi therapy could be identified, overall disease stabilization or uniform tumor regression leading to clinical remission was not observed. Moreover, only cases of tumor growth deceleration could be observed for melanomas after cessation of single-agent BRAFi therapy. Thus, the drug addiction phenotype can be readily elicited in DDR cell lines only if MAPK inhibition was reversed acutely and completely, and additional factors may modulate or mitigate this phenotype clinically.

Given the strong degree of double-drug addiction noted with both DDR4 and DDR5, we asked whether this would be generalizable across different cellular contexts and to melanoma cells with acquired resistance to BRAFi treatment alone. Interestingly, we found that melanoma cell lines adapted to growth with BRAFi+MEKi far more consistently displayed drug addiction (Figure 7D). Also consistent was the observation that melanoma cell lines with DDR displayed a greater rebound in p-ERK levels after drug washout (Figure 7E). This greater rebound was not necessarily due to the maximal p-ERK levels upon withdrawal of drugs but rather due to the very low p-ERK levels in the presence of both drugs (i.e., stronger on-target pathway suppression). Quantification of the fold changes in p-ERK levels (Figure 7E) and in clonogenic growths (Figure 7D) showed that they are strongly negatively correlated. Thus, melanoma cells with DDR displayed a stronger rebound in p-ERK levels and drug addiction upon drug withdrawal, when compared to melanoma cells with single-drug resistance withdrawn from BRAFi (Figure 7F). This p-ERK rebound is indicative of drug addiction since a suboptimal dose of ERKi could rescue

cells from double-drug withdrawal-induced loss of fitness (Figure 7C).

DISCUSSION

The understanding of how *BRAF* mutant melanomas frequently acquire BRAFi resistance via several distinct mechanisms, which thematically reactivate the MAPK pathway, has provided foundational rationale to combined BRAF/MEK inhibition to suppress such mechanisms. The ensuing translational effort has led to this combination supplanting BRAFi monotherapy in the clinic. This study of genetic alterations in melanomas with acquired BRAFi+MEKi resistance has provided unexpected insights. First, we detected alterations affecting similar genes known to be responsible for acquired BRAFi resistance, which suggests that the gene dosage or concurrence of these mutations may impart altered molecular interactions promoting BRAFi+MEKi resistance. The exaggerated genetic configurations encompassed gain-of-function (e.g., ^{V600E}*BRAF* ultra-amplification, ^{G12R}*NRAS* amplification) and LOF (e.g., ^{F127V}*PTEN*, deletions affecting *PTEN*, *CDKN2A*, *DUSP4*) alterations, and their combinations. Second, focusing on MAPK reactivation, we uncovered a highly plastic or tunable RAF-MEK complex resulting from mutations (single-nucleotide variants [SNVs] and/or CNVs). For instance, supraphysiologic levels of ^{V600E}*BRAF* allosterically relay oncogenic MAPK signaling via back-to-back interactions with CRAF. Moreover, moderately overexpressed levels of ^{V600E}*BRAF* likely regulate MEK1 and MEK2 activation via a face-to-face complex. These altered molecular interactions underscore an intrinsic limitation of combined BRAF and MEK inhibition and predict potential limitations of further downstream inhibitors (e.g., ERKi) in overcoming acquired BRAFi+MEKi resistance.

Thus, we have shown how (1) quantitative genetic alterations or gene dosage impact qualitative modes of signaling and (2) combinatorial alterations might be selected to impact survival signaling cooperatively (Figure 8). MEK1 and MEK2 mutants with alterations residing in or proximal to the helices A and C substructures share an increased ability to form an activation-associated complex with ^{V600E}*BRAF*, especially when both BRAF and MEK mutants are moderately overexpressed. Moreover, a proposed ^{MUT}MEK-^{V600E}*BRAF* heterodimer interface strongly suggests that such a face-to-face physical interaction involves predominantly a kinase-independent or regulatory function of ^{V600E}*BRAF*. Together, these data indicate a ^{V600E}*BRAF*-CRAF-MEK signaling complex that is highly susceptible to upregulation via single or multiple convergent genetic (and likely nongenetic) alterations.

Our study of melanoma cell lines with acquired resistance to combined BRAF and MEK inhibition has revealed insights into recent clinical studies. For instance, melanoma cell lines with preexisting BRAFi resistance augment preexisting mechanisms quickly as they adapt to combined BRAF and MEK inhibition. This is consistent with the clinical observation that patients who progressed on BRAFi or MEKi monotherapies infrequently respond to the addition of the other inhibitor, and, for those who do respond sequentially, the responses are generally highly transient. Furthermore, the importance of an MAPKi resistance-related complex has certain translational implications. Successful strategies targeting

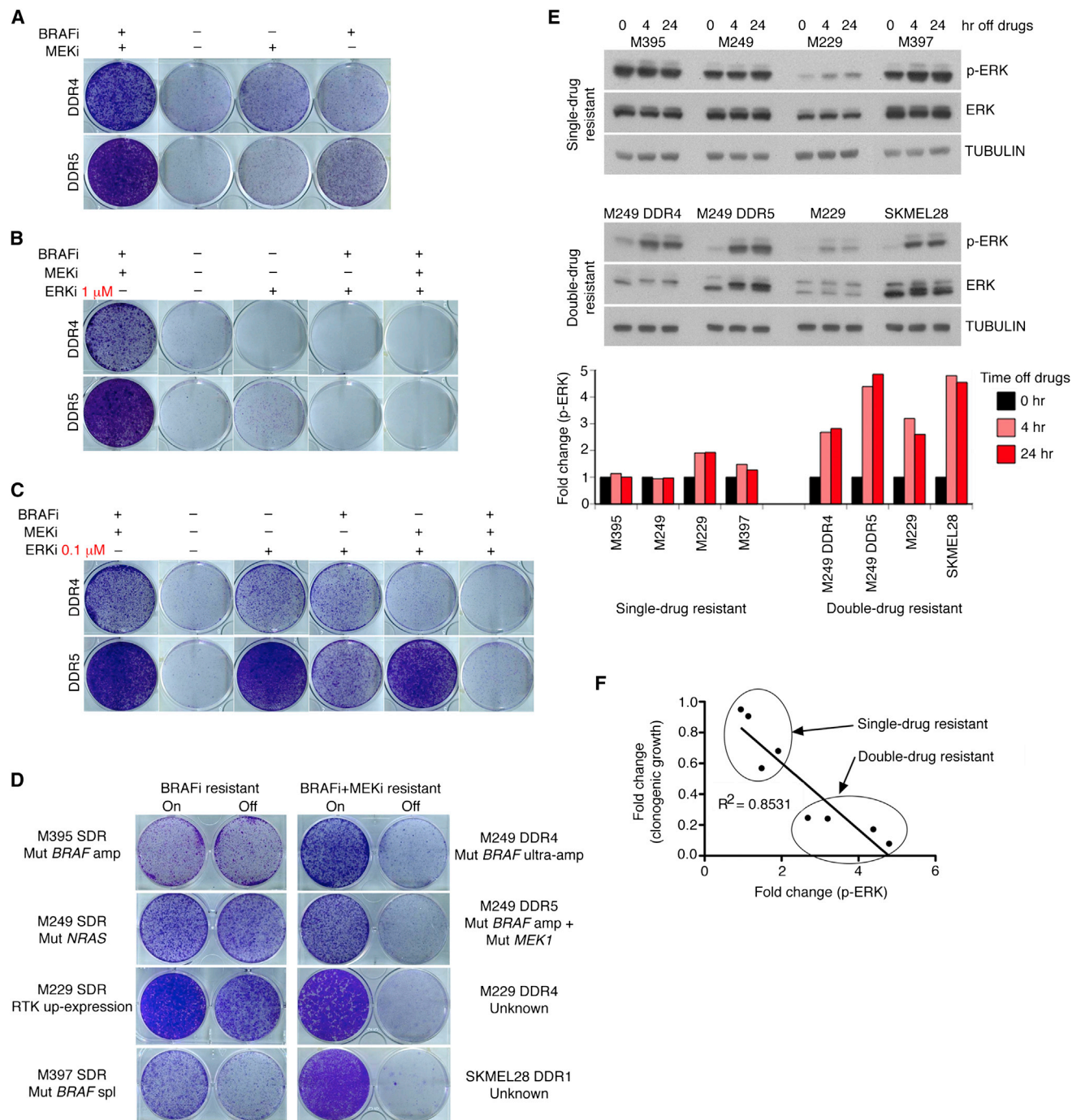


Figure 7. Resistance to Combined BRAF/MEK Inhibition Results in Exquisite Drug Addiction

(A) Clonogenic survival of M249 DDR cell lines plated in BRAFⁱ+MEKi, 1 μ M each, for 72 hr and then cultured for 9 days with or without specific inhibitor withdrawal (representative of three independent repeats).

(B and C) Clonogenic assays as in (A) except for the indicated high (B) or low (C) ERKi doses starting at 72 hr after plating.

(D) Clonogenic assays comparing SDR versus DDR cell lines of distinct genetic backgrounds and resistance mechanisms. amp, amplification; spl, splicing.

(E) WB analysis of p-ERK levels without or with acute BRAFⁱ (SDR) or BRAFⁱ+MEKi (DDR) withdrawal for 4 and 24 hr. TUBULIN, loading control. Quantification of p-ERK signals normalized to TUBULIN levels is shown for each cell line relative to the baseline signals (no inhibitor withdrawal).

(F) Correlation between changes in p-ERK levels (E, 4 versus 0 hr) and in clonogenic growths (D) upon inhibitor(s) withdrawal.

BRAFⁱ, vemurafenib; MEKi, selumetinib; ERKi, SCH72984. See also Figure S6 and Table S4.

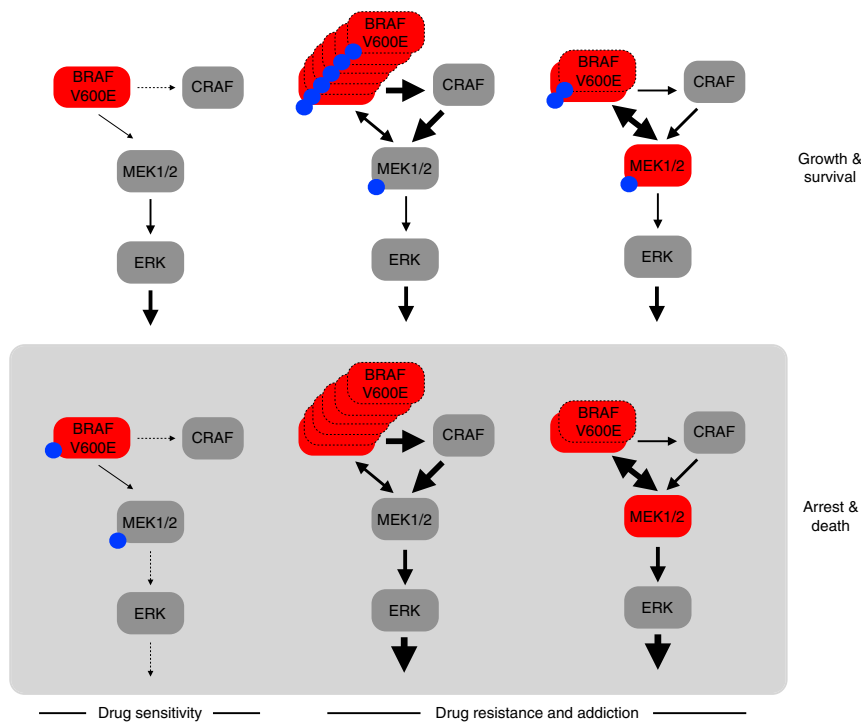


Figure 8. Alterations in a $V600E$ BRAF-CRAF-MEK Complex with Opposite Impacts on Melanoma Fitness Contingent on the Presence of BRAF and MEK Inhibitors

Alternative configurations of an RAF-MEK resistance-related complex consisting of (1) a supra-physiologic level of $V600E$ BRAF, which activates CRAF, or (2) a moderately overexpressed $V600E$ BRAF level concomitant with a mutant MEK1 (or MEK2), which leads to increased $V600E$ BRAF- MUT MEK interaction. Both signaling configurations strongly favor ERK activation, leading to growth and survival finely tuned to the BRAFi+MEKi level. Paradoxically, acute removal of BRAFi+MEKi disrupts this fine-tuning and results in a p-ERK rebound favoring cell arrest and death (i.e., drug addiction). WT (gray) and mutant (red) proteins; blue circles, BRAFi or MEKi.

University of California, San Francisco; and Vanderbilt-Ingram Cancer Center and informed consents of each patient. Patients were enrolled in GlaxoSmithKline or Roche/Genentech clinical trials or treated per standard clinical management. We evaluated 45 tumor samples (27 DD-DP, 4 DP, and 14 baseline or early on-treatment melanoma biopsies) from 14 patients who were either treated with BRAFi+MEKi upfront or with this combination

this tunable-combinatorial signaling complex may include those inhibiting CRAF function (e.g., omni- or pan-RAF inhibitors), $V600E$ BRAF-CRAF interaction, $V600E$ BRAF- MUT MEK interaction or scaffolding, and MEK activation (e.g., phosphorylation by RAF). These strategies could be built around continued inhibition of mutant BRAF and MEK or alternating regimens. In our studies, the efficacy of an ERK inhibitor in overcoming acquired BRAFi+MEKi resistance was nuanced and depended on the experimental contexts, e.g., ERKi alone at lower concentrations promoted survival and growth of BRAFi+MEKi-resistant melanoma cells in both short- and long-term assays.

While the buildup of a $V600E$ BRAF-CRAF-MEK complex ultimately limited the efficacy of combined BRAF and MEK inhibition in melanoma, this signaling complex appeared to be poised to deliver a lethal dose of signaling once both inhibitors were efficiently and acutely removed (Figure 8). Melanoma cells with fully acquired BRAFi+MEKi resistance were much more sensitive to drug withdrawal than those with acquired resistance to BRAFi alone. It is possible that in vivo factors, such as tumor heterogeneity (e.g., subpopulations with reversible drug tolerance but without drug addiction), 3D cell-cell contacts, microenvironmental signals, and/or host pharmacokinetic considerations, could render drug addiction a clinically intractable phenotype. In this light, the hypothesis of intermittent therapy with combined BRAFi and MEKi to delay acquired resistance will be tested prospectively within a large randomized clinical trial (SWOG/CTEP S1320) for the treatment of patients with BRAF mutant metastatic melanoma.

EXPERIMENTAL PROCEDURES

Patients, Tumor Samples, and Genomic Analysis

Melanoma tissues and patient-matched normal tissues were collected with the approval of institutional review boards at University of California, Los Angeles;

after progression on BRAFi. In each tumor, genetic mechanisms (excluding PI3K-PTEN-AKT genetic hits) known to confer clinical resistance to BRAFi were detected by gDNA qPCR and/or Sanger sequencing. Twenty-three baseline and DD-DP tumors from seven patients along with normal tissues were WES analyzed to detect somatic alterations that are in the MAPK and PI3K-PTEN-AKT pathways and that are specific to drug-resistant tumors. Pair-end sequences with read length of 2x100 base pairs using the Illumina HiSeq2000 platform were generated. SNVs, insertion-deletions (INDELs), and CNVs were analyzed and visualized as described previously (Shi et al., 2014).

Targeted Sequencing, Copy-Number Quantification, and WES of Cell Lines

BRAF, NRAS, and DUSP4 cDNA levels were quantified by real-time RT-PCR using TUBULIN and GAPDH levels for normalization. Relative expressions were calculated using the delta-Ct method. BRAF, NRAS, and DUSP4 gDNA relative copy numbers were quantified by real-time PCR with total gDNA content estimated by assaying the β -globin gene in each sample. All primer sequences are available upon request. Sanger sequencing was performed using purified PCR via BigDye v1.1 (Applied Biosystems) in combination with a 3730 DNA Analyzer (Applied Biosystems). WES of M249 triple cell lines were analyzed for shared and distinct genetic alterations and their phylogenetic relationship.

Cell Culture, Constructs, Infections, and Transfections

All cell lines were maintained in DMEM with 10% heat-inactivated fetal bovine serum, 2 mmol/l glutamine in a humidified 5% CO₂ incubator, with the addition of 10 ng/ml doxycycline and/or puromycin, when applicable. Stocks and dilutions of PLX4032/vemurafenib (Plexxikon), AZD6244/selumetinib (Selleck Chemicals), and SCH722984 (Merck) were made in DMSO. Cell proliferation experiments were performed in a 96-well format (five replicates per sample), drug treatments were initiated 24 hr postseeding for 72 hr, and cell survival was quantified using CellTiter-GLO assay (Promega). Clonogenic assays were performed by plating cells at single-cell density in six-well plates with fresh media and drug replenished every 2 days. Colonies were fixed in 4% paraformaldehyde and stained with 0.05% crystal violet. shBRAF, shCRAF, shPTEN, and shNRAS were subcloned into the lentiviral vector pLL3.7; shDUSP4/pLK0.1 vectors were obtained commercially (Dharmacon). All WT and mutant MEK1 and BRAF constructs were epitope tagged and subcloned into the doxycycline-repressible lentiviral vector pLVX-Tight-Puro

(Clontech Laboratories). Viral supernatants were generated by third-generation lentiviral packaging using HEK293T cells. HEK293T cells were transfected using BioT (Bioland).

Protein Detection, Interaction, and Structure

Cell lysates were made in radioimmunoprecipitation assay buffer (Sigma) for direct western blotting or in a PNE buffer (PBS:H₂O at 1:1, 0.5% Nonidet P-40, 5 mM EDTA, and 5% glycerol) for immunoprecipitation, with both buffers supplemented with protease (Roche) and phosphatase (Santa Cruz Biotechnology) inhibitor cocktails. Western blots and immunoprecipitations were performed using the following antibodies: p-ERK1/2 (T202/Y204), p-MEK1/2 (S217/221), p-AKT (T308), p-CRAF (S338), total ERK1/2, MEK1/2, MEK1, MEK2, AKT, CRAF, DUSP4, and HA (Cell Signaling Technology); TUBULIN and FLAG (Sigma); BRAF (F-7), BRAF (C-19), p-MEK1 (T291), and p-MEK1 (S222) (Santa Cruz); and p-MEK2 (S226) (United States Biological). Western blot quantification was performed using NIH ImageJ. The 3D structures of MEK1 (3EQC) and PTEN mutants were modeled by the I-TASSER online server. Modeling the ^{V600E}BRAF-^{WT}MEK1 dimer interface was based on the crystal structure of the ^{WT}BRAF-^{WT}MEK1 dimer (4MNE); the MEK1-KSR2 dimer (2Y4I); and the asymmetric, vemurafenib-bound ^{V600E}BRAF dimer (3G07). Protein structures were visualized using PyMol (DeLano Scientific).

ACCESSION NUMBERS

The Sequence Read Archive accession number for the exome sequence data reported in this paper is SRP049746.

SUPPLEMENTAL INFORMATION

Supplemental Information includes six figures, four tables, and one movie and can be found with this article online at <http://dx.doi.org/10.1016/j.ccell.2014.11.018>.

AUTHOR CONTRIBUTIONS

G.M., W.H., A.H., H. Shi, X.K., C.C.Y., and R.S.L. designed and performed experiments and analyzed data. R.C.K., A.A.S., N.K., J.B., K.B.D., D.B.J., A.A., J.A.S., A.R., and R.S.L. contributed clinical samples or key reagents. K.R., H. Seifert, J.L., D.B.J., A.A., J.A.S., A.R., and R.S.L. analyzed clinical data. R.S.L. wrote the paper. G.M., W.H., A.H., H.S., X.K., D.B.J., A.A., J.A.S., and A.R. contributed to writing the paper. G.M., W.H., A.H., and H. Shi contributed equally to this work.

ACKNOWLEDGMENTS

We are grateful to G. Bollag (Plexxikon) for providing PLX4032; B. Chmielowski and J. Glaspy for coordinated patient care; Art Villanueva, Jackie Hernandez, Elizabeth Seja, and Christine Kivork for coordinating clinical trials and specimen collection; Donald Hucks for his technical assistance; and all patient volunteers. This work has been funded by Burroughs Wellcome Fund (to R.S.L.), Stand Up To Cancer (to R.S.L.), Melanoma Research Alliance (to R.S.L. and A.A.), the NIH (1R01CA176111 to R.S.L., 1P01CA168585 to A.R. and R.S.L., 5K24CA097588-09 to J.A.S.), the Ressler Family Foundation (to R.S.L. and A.R.), the Seaver institute (to R.S.L. and A.R.), the American Skin Association (to H. Shi and R.S.L.), the Harry J. Lloyd Charitable Trust (to R.S.L.), the Ian Copeland Melanoma Fund (to R.S.L.), the Steven C. Gordon Family Foundation (to R.S.L. and A.R.), the T. J. Martell Foundation (to K.B.D.), the Robert J. Kleberg, Jr. and Helen C. Kleberg Foundation (to K.B.D.), and the Royal Marsden (to J.L.).

Received: April 22, 2014

Revised: September 1, 2014

Accepted: November 19, 2014

Published: January 15, 2015

REFERENCES

Bollag, G., Hirth, P., Tsai, J., Zhang, J., Ibrahim, P.N., Cho, H., Spevak, W., Zhang, C., Zhang, Y., Habets, G., et al. (2010). Clinical efficacy of a RAF inhib-

itor needs broad target blockade in BRAF-mutant melanoma. *Nature* **467**, 596–599.

Brennan, D.F., Dar, A.C., Hertz, N.T., Chao, W.C., Burlingame, A.L., Shokat, K.M., and Barford, D. (2011). A Raf-induced allosteric transition of KSR stimulates phosphorylation of MEK. *Nature* **472**, 366–369.

Catalanotti, F., Reyes, G., Jesenberger, V., Galabova-Kovacs, G., de Matos Simoes, R., Carugo, O., and Baccarini, M. (2009). A Mek1-Mek2 heterodimer determines the strength and duration of the Erk signal. *Nat. Struct. Mol. Biol.* **16**, 294–303.

Corcoran, R.B., Dias-Santagata, D., Bergethon, K., Iafrate, A.J., Settleman, J., and Engelman, J.A. (2010). BRAF gene amplification can promote acquired resistance to MEK inhibitors in cancer cells harboring the BRAF V600E mutation. *Sci. Signal.* **3**, ra84.

Emery, C.M., Vijayendran, K.G., Zipser, M.C., Sawyer, A.M., Niu, L., Kim, J.J., Hattori, C., Chopra, R., Oberholzer, P.A., Karpova, M.B., et al. (2009). MEK1 mutations confer resistance to MEK and B-RAF inhibition. *Proc. Natl. Acad. Sci. USA* **106**, 20411–20416.

Haling, J.R., Sudhamsu, J., Yen, I., Sideris, S., Sandoval, W., Phung, W., Bravo, B.J., Giannetti, A.M., Peck, A., Masselot, A., et al. (2014). Structure of the BRAF-MEK complex reveals a kinase activity independent role for BRAF in MAPK signaling. *Cancer Cell* **26**, 402–413.

Hodis, E., Watson, I.R., Kryukov, G.V., Arold, S.T., Imielinski, M., Theurillat, J.P., Nickerson, E., Auclair, D., Li, L., Place, C., et al. (2012). A landscape of driver mutations in melanoma. *Cell* **150**, 251–263.

Krauthammer, M., Kong, Y., Ha, B.H., Evans, P., Bacchicocchi, A., McCusker, J.P., Cheng, E., Davis, M.J., Goh, G., Choi, M., et al. (2012). Exome sequencing identifies recurrent somatic RAC1 mutations in melanoma. *Nat. Genet.* **44**, 1006–1014.

Nan, X., Collisson, E.A., Lewis, S., Huang, J., Tamgüney, T.M., Liphardt, J.T., McCormick, F., Gray, J.W., and Chu, S. (2013). Single-molecule superresolution imaging allows quantitative analysis of RAF multimer formation and signaling. *Proc. Natl. Acad. Sci. USA* **110**, 18519–18524.

Nazarian, R., Shi, H., Wang, Q., Kong, X., Koya, R.C., Lee, H., Chen, Z., Lee, M.K., Attar, N., Sazegar, H., et al. (2010). Melanomas acquire resistance to B-RAF(V600E) inhibition by RTK or N-RAS upregulation. *Nature* **468**, 973–977.

Nikolaev, S.I., Rimoldi, D., Iseli, C., Valsesia, A., Robyr, D., Gehrig, C., Harshman, K., Guipponi, M., Bukach, O., Zoete, V., et al. (2012). Exome sequencing identifies recurrent somatic MAP2K1 and MAP2K2 mutations in melanoma. *Nat. Genet.* **44**, 133–139.

Poulikakos, P.I., Persaud, Y., Janakiraman, M., Kong, X., Ng, C., Moriceau, G., Shi, H., Atefi, M., Titz, B., Gabay, M.T., et al. (2011). RAF inhibitor resistance is mediated by dimerization of aberrantly spliced BRAF(V600E). *Nature* **480**, 387–390.

Ribas, A., and Flaherty, K.T. (2011). BRAF targeted therapy changes the treatment paradigm in melanoma. *Nat. Rev. Clin. Oncol.* **8**, 426–433.

Shi, H., Moriceau, G., Kong, X., Koya, R.C., Nazarian, R., Pupo, G.M., Bacchicocchi, A., Dahlman, K.B., Chmielowski, B., Sosman, J.A., et al. (2012a). Preexisting MEK1 exon 3 mutations in V600E/KBRAF melanomas do not confer resistance to BRAF inhibitors. *Cancer Discov.* **2**, 414–424.

Shi, H., Moriceau, G., Kong, X., Lee, M.K., Lee, H., Koya, R.C., Ng, C., Chodon, T., Scolyer, R.A., Dahlman, K.B., et al. (2012b). Melanoma whole-exome sequencing identifies (V600E)B-RAF amplification-mediated acquired B-RAF inhibitor resistance. *Nat. Commun.* **3**, 724.

Shi, H., Hugo, W., Kong, X., Hong, A., Koya, R.C., Moriceau, G., Chodon, T., Guo, R., Johnson, D.B., Dahlman, K.B., et al. (2014). Acquired resistance and clonal evolution in melanoma during BRAF inhibitor therapy. *Cancer Discov.* **4**, 80–93.

Thakur, M.D., Salangsang, F., Landman, A.S., Sellers, W., Pryer, N.K., Levesque, M.P., Dummer, R., McMahon, M., and Stuart, D.D. (2013). Modeling vemurafenib resistance in melanoma reveals a strategy to forestall drug resistance. *Nature* **494**, 251–255.

Van Allen, E.M., Wagle, N., Sucker, A., Treacy, D.J., Johannessen, C.M., Goetz, E.M., Place, C.S., Taylor-Weiner, A., Whittaker, S., Kryukov, G.V., et al.; Dermatologic Cooperative Oncology Group of Germany (DeCOG)

- (2014). The genetic landscape of clinical resistance to RAF inhibition in metastatic melanoma. *Cancer Discov.* 4, 94–109.
- Villanueva, J., Infante, J.R., Krepler, C., Reyes-Urbe, P., Samanta, M., Chen, H.Y., Li, B., Swoboda, R.K., Wilson, M., Vultur, A., et al. (2013). Concurrent MEK2 mutation and BRAF amplification confer resistance to BRAF and MEK inhibitors in melanoma. *Cell Rep.* 4, 1090–1099.
- Wagle, N., Emery, C., Berger, M.F., Davis, M.J., Sawyer, A., Pochanard, P., Kehoe, S.M., Johannessen, C.M., Macconail, L.E., Hahn, W.C., et al. (2011). Dissecting therapeutic resistance to RAF inhibition in melanoma by tumor genomic profiling. *J. Clin. Oncol.* 29, 3085–3096.
- Wagle, N., Van Allen, E.M., Treacy, D.J., Frederick, D.T., Cooper, Z.A., Taylor-Weiner, A., Rosenberg, M., Goetz, E.M., Sullivan, R.J., Farlow, D.N., et al. (2014). MAP kinase pathway alterations in BRAF-mutant melanoma patients with acquired resistance to combined RAF/MEK inhibition. *Cancer Discov.* 4, 61–68.
- Wang, H., Daouti, S., Li, W.H., Wen, Y., Rizzo, C., Higgins, B., Packman, K., Rosen, N., Boylan, J.F., Heimbrook, D., and Niu, H. (2011). Identification of the MEK1(F129L) activating mutation as a potential mechanism of acquired resistance to MEK inhibition in human cancers carrying the B-RafV600E mutation. *Cancer Res.* 71, 5535–5545.